

# Rare Coding Variants in *ANGPTL6* Are Associated with Familial Forms of Intracranial Aneurysm

Romain Bourcier,<sup>1,2</sup> Solena Le Scouarnec,<sup>1</sup> Stéphanie Bonnaud,<sup>1,3</sup> Matilde Karakachoff,<sup>1,3</sup> Emmanuelle Bourcereau,<sup>3</sup> Sandrine Heurtebise-Chrétien,<sup>1</sup> Céline Menguy,<sup>1</sup> Christian Dina,<sup>1,3</sup> Floriane Simonet,<sup>1,3</sup> Alexis Moles,<sup>4</sup> Cédric Lenoble,<sup>2</sup> Pierre Lindenbaum,<sup>1</sup> Stéphanie Chatel,<sup>1,3</sup> Bertrand Isidor,<sup>5</sup> Emmanuelle Génin,<sup>6</sup> Jean-François Deleuze,<sup>7</sup> Jean-Jacques Schott,<sup>1,3</sup> Hervé Le Marec,<sup>1,3</sup> ICAN Study Group, Gervaise Loirand,<sup>1,3,8</sup> Hubert Desal,<sup>1,2,8,\*</sup> and Richard Redon<sup>1,3,8,\*</sup>

Intracranial aneurysms (IAs) are acquired cerebrovascular abnormalities characterized by localized dilation and wall thinning in intracranial arteries, possibly leading to subarachnoid hemorrhage and severe outcome in case of rupture. Here, we identified one rare nonsense variant (c.1378A>T) in the last exon of *ANGPTL6* (Angiopoietin-Like 6)—which encodes a circulating pro-angiogenic factor mainly secreted from the liver—shared by the four tested affected members of a large pedigree with multiple IA-affected case subjects. We showed a 50% reduction of *ANGPTL6* serum concentration in individuals heterozygous for the c.1378A>T allele (p.Lys460Ter) compared to relatives homozygous for the normal allele, probably due to the non-secretion of the truncated protein produced by the c.1378A>T transcripts. Sequencing *ANGPTL6* in a series of 94 additional index case subjects with familial IA identified three other rare coding variants in five case subjects. Overall, we detected a significant enrichment ( $p = 0.023$ ) in rare coding variants within this gene among the 95 index case subjects with familial IA, compared to a reference population of 404 individuals with French ancestry. Among the 6 recruited families, 12 out of 13 (92%) individuals carrying IA also carry such variants in *ANGPTL6*, versus 15 out of 41 (37%) unaffected ones. We observed a higher rate of individuals with a history of high blood pressure among affected versus healthy individuals carrying *ANGPTL6* variants, suggesting that *ANGPTL6* could trigger cerebrovascular lesions when combined with other risk factors such as hypertension. Altogether, our results indicate that rare coding variants in *ANGPTL6* are causally related to familial forms of IA.

## Introduction

Intracranial aneurysms (IAs) are acquired cerebrovascular abnormalities affecting 3% of the general population, at a mean age of 50 years.<sup>1</sup> They are characterized by a localized dilation and wall thinning in typical locations in intracranial arteries.<sup>2</sup> The most notorious and deleterious complication of an IA is the rupture, resulting in subarachnoid hemorrhage that can lead to severe disability and death.<sup>3</sup> Neither reliable biomarkers nor diagnostic tools are currently available to predict IA formation or evolution. Current treatments are mostly invasive and rely on microsurgical or endovascular treatment with a risk of procedural morbidity or mortality.<sup>4</sup>

Although the pathogenesis of IAs has been the subject of several studies for many years, the mechanisms underlying their formation, growth, and eventual rupture remain largely unknown.<sup>5</sup> IAs are mostly acquired lesions resulting from a defective vascular wall response to local hemodynamic stress.<sup>6</sup> The structural deterioration of the arterial wall involves inflammation and tissue degeneration with degradation of the extracellular matrix and smooth muscle cell apoptosis.<sup>7</sup> Risk factors such as hypertension, female sex, increasing age, smoking, excessive alcohol consumption, and familial history of aneurysm predispose to IA

formation and rupture.<sup>8</sup> Furthermore, increasing evidence suggests a genetic component of IA formation.<sup>9</sup> Genome-wide association studies and subsequent case-control replication analyses have identified common risk alleles for IA formation, in particular on chromosome 9 within the cyclin-dependent kinase inhibitor 2B antisense inhibitor gene, on chromosome 8 near the transcription regulator gene *SOX17*, and on chromosome 4 near the endothelin receptor A gene.<sup>10</sup> However, these loci altogether may only explain around 5% of familial risk in Europe and Japan.<sup>11</sup>

Whole-exome sequencing approaches have recently been applied to families with multiple IA-affected case subjects, leading to the identification of genes associated with IA pathogenesis susceptibility, such as *RNF213* (MIM: 613768)<sup>12</sup> or *THSD1* (MIM: 616821).<sup>13</sup> While the Ring Finger Protein 213 had been previously involved in vascular-wall construction,<sup>14,15</sup> inactivation of the Thrombospondin Type 1 Domain Containing Protein 1 has been reported to impair the adhesion of endothelial cells to the extracellular matrix and to cause cerebral bleeding and increased mortality in zebrafish and mice.<sup>13</sup> These recent advances provide new insights into the pathophysiology of IA and demonstrate the usefulness of familial approaches based on whole-exome sequencing to improve

<sup>1</sup>INSERM, CNRS, UNIV Nantes, l'institut du thorax, 44007 Nantes, France; <sup>2</sup>Department of Neuroradiology, CHU Nantes, 44093 Nantes, France; <sup>3</sup>CHU Nantes, l'institut du thorax, 44093 Nantes, France; <sup>4</sup>Department of Neurosurgery, CHU Nantes, 44093 Nantes, France; <sup>5</sup>Department of Medical Genetics, CHU Nantes, 44093 Nantes, France; <sup>6</sup>Université de Bretagne Occidentale, Inserm UMR 1078, Centre Hospitalier Régional Universitaire de Brest, Etablissement Français du Sang, 29238 Brest, France; <sup>7</sup>Centre National de Recherche en Génomique Humaine, CEA, 91057 Evry, France

<sup>8</sup>These authors contributed equally to this work

\*Correspondence: [hubert.desal@chu-nantes.fr](mailto:hubert.desal@chu-nantes.fr) (H.D.), [richard.redon@inserm.fr](mailto:richard.redon@inserm.fr) (R.R.)

<https://doi.org/10.1016/j.ajhg.2017.12.006>

© 2017 American Society of Human Genetics.



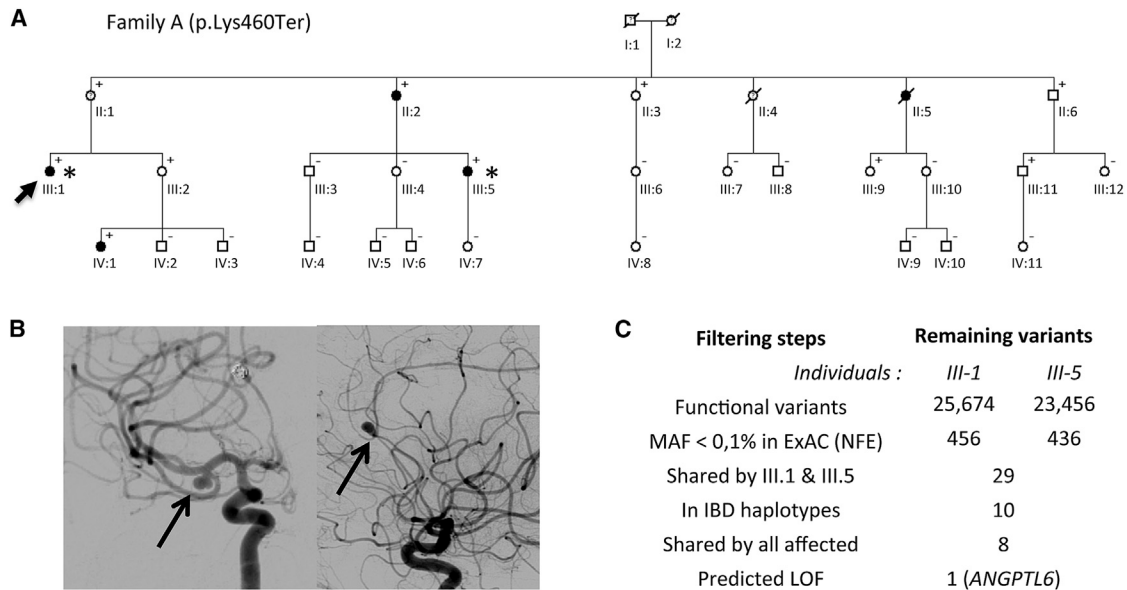


**Figure 1. Genetic Investigations in a Large Family with Multiple IA-Affected Case Subjects**

(A) Pedigree of family A showing the segregation pattern of the variant *ANGPTL6* c.1378A>T. Filled boxes, empty boxes, and boxes with question marks indicate IA-affected case subjects, non-affected relatives, and individuals with unknown status; plus sign (+) indicates the presence of the *ANGPTL6* variant; minus sign (-) indicates its absence; arrow indicates the index case subject; and asterisks indicate the individuals included in WES analysis.

(B) Digital subtracted angiographies showing two intracranial aneurysms carried by the index case III-1, one on the middle cerebral artery (left) and one on the anterior cerebral artery (right).

(C) Summary of the filtering steps applied to genetic variants detected by WES in individuals III-1 and III-5. Abbreviations: MAF, minor allele frequency; IBD, identity by descent; LOF, loss of function.

knowledge on the molecular mechanisms underlying IA formation and rupture.

In the present study, by combining whole-exome sequencing, identity-by-descent (IBD) analysis, gene burden testing, and functional investigations, we identified rare coding variants in the angiopoietin-like 6 gene (*ANGPTL6* [MIM: 609336]) as causally related to familial forms of IA.

## Material and Methods

### Clinical Recruitment

Familial cases of IA are defined as at least two first-degree relatives both diagnosed with typical IA (defined as a saccular arterial dilatation of any size occurring at a bifurcation of the intracranial vasculature), without any age limitation. Index case subjects and their relatives were recruited following the French ethical guidelines for genetic research and under approval from the French Ministry of Research (no. DC-2011-1399) and the local ethical committee. Informed written consent was obtained from each individual agreeing to participate in the genetic study, to whom MRI screening and blood sampling were proposed.

The full recruiting process has been described previously.<sup>16</sup> In brief, neuroradiological phenotyping was performed in each recruiting center by interventional neuroradiologists, neurologists, and neurosurgeons in order to recruit only case subjects with typical saccular bifurcation IA. Mycotic, fusiform-shaped, or dissecting IAs were systematically excluded, as well as IA in relation with an arteriovenous malformation and IA resulting from syndromic disorders such as Marfan disease or vascular forms

of Ehlers Danlos. Eye fundus, transthoracic echocardiography, non-invasive analysis of endothelial dysfunction, and Doppler echography analysis of peripheral arteries (sub clavians, radials, femorals, renals, and digestives) were carried out to check for any other vascular malformation or variation potentially linked to the presence of IA, thus constituting a syndrome yet unknown.

### Whole-Exome Sequencing (WES)

Genomic DNA was extracted from peripheral blood lymphocytes using the NucleoSpin Blood kit XL (Macherey Nagel). In brief, coding exons from 3  $\mu$ g of genomic DNA were captured using the SureSelect Human All Exon V4 Kit (Agilent Technologies), following the manufacturer's protocol. DNA was sheared by acoustic fragmentation (Bioruptor Diagenode) and purified with the magnetic beads Agencourt AMPure XP (Beckmann Coulter genomics), and fragment quality was assessed (TapeStation 2200 Agilent). Exome-enriched genomes were paired-end sequenced (100-bp reads) on Illumina HiSeq 1500 (Illumina) to a mean depth above 30 $\times$ . Sequence reads were mapped to the human reference genome (Broad Institute human\_g1k\_v37) using the Burrows-Wheeler Aligner.<sup>17</sup> Duplicates were flagged using Picard software. Reads were realigned and recalibrated using the Genome Analysis Toolkit (GATK).<sup>18</sup> Variant detection was performed with GATK HaplotypeCaller. Functional annotation of high-quality variants was performed using Ensembl VEPv7.4. The sequencing quality was determined with the Depth Of Coverage Walker provided in GATK. Knime4Bio<sup>19</sup> was used for all merging and filtering steps. Variants with a sequencing depth of less than 10 or a genotype quality below 90 were excluded, as well as synonymous variants with no predicted effect on splicing sites. At last, from the resulting set of "functional" variants (as reported in Figure 1), we filtered

out any variant with a minor allele frequency (MAF) higher than 0.1% in the non-Finnish European (NFE) population from the ExAC database, as well as few remaining variants reported with a minor allele frequency (MAF) higher than 10% in our in-house database of 260 whole-exome sequences from individuals with various cardiac phenotypes.

### Identity-by-Descent Analysis

SNP genotyping was performed on population-optimized Affymetrix Axiom Genome-Wide CEU 1 array plates following the standard manufacturer's protocol. Fluorescence intensities were quantified using the Affymetrix GeneTitan Multi-Channel Instrument, and primary analysis was conducted with Affymetrix Power Tools following the manufacturer's recommendations. After genotype calling, all individuals had a genotype call rate above 97%. SNPs with an MAF < 10%, a call rate < 95%, or  $p < 1 \times 10^{-5}$  when testing for Hardy-Weinberg equilibrium were excluded. IBD estimation was performed with IBDLD v.3.34, NoLD method.<sup>20</sup> Shared regions were obtained by analyzing a set of independent SNPs ( $R^2 < 0.2$ ) using genotypes from French individuals<sup>21</sup> as a reference panel. The IBD status at every SNP locus was obtained for each pair of individuals, based on a hidden Markov model implemented in the IBDLD program. Still using IBDLD, we estimated the kinship coefficients between pairs of IA-affected case subjects from distinct pedigrees. We invariably found values around 0.025, thus excluding non-documented close relatedness between individuals from distinct pedigrees carrying the same rare variant in *ANGPTL6*.

### Capillary Sequencing and Burden Testing

Validation experiments for each selected variant, familial segregation analyses, and further screening for *ANGPTL6* coding mutations were performed by capillary sequencing on an Applied Biosystems 3730 DNA Analyzer, using standard procedures. Sequence analyses were performed with SeqScape v.2.5. *ANGPTL6* variants were numbered according to the canonical transcript (GenBank: NM\_031917.2). Burden test was performed using SKAT<sup>22</sup> and CAST,<sup>23</sup> by comparing the proportion of individuals carrying at least one rare coding variant within *ANGPTL6* among the 95 index case subjects with IA versus 404 healthy individuals with French ancestry. *ANGPTL6* status in control individuals was determined by whole-genome sequencing with a mean depth of coverage above 30 $\times$ . Rare variants were defined as variants with an MAF below 1% among the 7,509 whole-genome-sequenced individuals with NFE ancestry from the gnomAD database. The count of alleles with rare coding variants in *ANGPTL6* among case subjects was also compared with the same allele count among the 7,509 whole-genome sequenced individuals with NFE ancestry from gnomAD,<sup>24</sup> through the use of Fisher's exact test.

### Expression Analyses of *ANGPTL6*

HEK293 cells were maintained in Dulbecco's modified Eagle's medium (DMEM) supplemented with 10% fetal bovine serum and 1% penicillin-streptomycin. Stable HEK293 cell lines were obtained by transfection of pcDNA3.1 vector encoding WT *ANGPTL6* and p.Lys460Ter *ANGPTL6* (G418 selection). Recombinant proteins are expressed as Nter-FLAG fusion proteins. In HEK293, recombinant human proteins were detected by both anti-FLAG (Sigma Aldrich, F-3165), anti-*ANGPTL6* antibodies raised against AA 114-130 of *ANGPTL6* (Adipogen, AG-25A-

0030), and ELISA (kit supplied by Adipogen). In human subjects, serum *ANGPTL6* levels were measured by ELISA. For transcript analysis, total RNA from stably transfected HEK293 cells was purified using Trizol (Life technology) according to the manufacturer's instructions and then reverse-transcribed. Real-time quantitative PCR was performed using the TaqMan 7900 Sequence Detection System (Applied Biosystems). Primers used to assess *ANGPTL6* mRNA expression were designed using the Primer Express 3.1 software (sequences available on request).

## Results

### A Nonsense Variant in *ANGPTL6* Shared by Family Members with IA

The index case subject of family A (individual III-1; Figure 1A) was diagnosed after a subarachnoid hemorrhage (SAH) at the age of 51. This event revealed a ruptured anterior cerebral artery aneurysm and a second middle cerebral artery aneurysm (Figure 1B). She completely recovered from the subarachnoid hemorrhage and because of known familial history of ruptured IAs (II-2, II-5), a systematic screening was performed among relatives. Her cousin (III-5) and her niece (IV-1) were both diagnosed with two and one IAs, respectively. Her uncle (II-4) had an episode suggestive of aneurysmal SAH at the age of 36 and died before a CT scan or angiography could be performed. Her mother (II-1), who carries an ectasia measuring less than 2 mm and diagnosed as uncertain,<sup>16</sup> was classified as phenotype unknown.

Clinical information was collected for 28 individuals from family A (Table S1). IA was diagnosed on CT angiography or conventional angiography. DNA was available for 27 of them (DNA was unavailable for II-5 who died in 1974 after a rupture of IA). Individuals with IAs (II-2, II-5, III-1, III-5, and IV-1) were all female. Noteworthy, all IA-affected case subjects except IV-1 suffered from high blood pressure.

We combined WES and IBD analysis to identify any rare genetic variant likely explaining this familial form of IA. Whole-exome sequencing applied to the first cousins III-1 and III-5 led to the detection of 25,674 and 23,456 functional sequence variants, respectively, in comparison to the human reference genome assembly (Figure 1C). After filtering out genetic variants reported with an MAF above 0.1% in the non-Finnish European (NFE) population from the ExAC database,<sup>24</sup> we ended up with 29 rare variants shared between the first cousins, which were all manually reviewed by visual inspection of sequence reads using the Integrative Genomics Viewer.<sup>25</sup>

In parallel, IBD analysis of the complete pedigree identified 12 haplotypes shared by the 4 affected relatives. Within these chromosomal intervals, individuals III.1 and III.5 shared 10 rare, non-synonymous variants (Figure 1C). By capillary sequencing, we determined that the 4 affected relatives share 8 of these variants (Table 1), among which one nonsense variant, c.1378A>T (p.Lys460Ter), was in *ANGPTL6*.

**Table 1. Rare Non-synonymous Variants Shared by All Affected Members in Family A, and Rare Non-synonymous Variants in *ANGPTL6* Detected in Other Families**

Family	Genomic Position (GRCh37/hg19)	Gene	Nucleotide Change <sup>a</sup>	Protein Consequence <sup>a</sup>	MAF in ExAC (NFE)	GERP Score	Predicted Functional Impact		Carriers / Total	
							SIFT	PolyPhen-2	Affected	Unaffected
A	chr6:52701135C>A	<i>GSTA5</i>	c.171G>T	p.Met57Ile	0.00002	2.63	deleterious	benign	4/4	5/22
A	chr10:73046467G>A	<i>UNC5B</i>	c.574G>A	p.Asp192Asn	0.00001	5.43	deleterious	possibly_damaging	4/4	10/22
A	chr11:64756981G>A	<i>BATF2</i>	c.373C>T	p.Leu125Phe	0.00002	3.54	tolerated	possibly_damaging	4/4	6/22
A	chr11:65113459G>T	<i>DPF2</i>	c.122G>T	p.Gly41Val	0.00013	-7.09	tolerated	unknown	4/4	6/22
A	chr11:65746304C>T	<i>SART1</i>	c.2303C>T	p.Thr768Ile	0.00000	4.76	deleterious	probably_damaging	4/4	6/22
A	chr19:10610439C>T	<i>KEAP1</i>	c.271G>A	p.Ala91Thr	0.00013	4.68	tolerated	benign	4/4	5/22
A	chr19:14001265G>A	<i>C19orf57</i>	c.404C>T	p.Ala135Val	0.00025	-3.41	deleterious	benign	4/4	5/22
A	chr19:10203300T>A	<i>ANGPTL6</i>	c.1378A>T	p.Lys460Ter	0.00001	4.39	LOF		4/4	5/22
B + C	chr19:10206848T>A	<i>ANGPTL6</i>	c.392A>T	p.Glu131Val	not found	4.03	deleterious	benign	4/4	4/10
D	chr19:10204205G>A	<i>ANGPTL6</i>	c.1042C>T	p.Leu348Phe	not found	3.67	tolerated	probably_damaging	1/1	0/1
E + F	chr19:10206782G>GC+	<i>ANGPTL6</i>	c.439_457dup	p.Ala153ValfsTer66	0.00060	4.36	LOF		3/4	6/8

Abbreviations are as follows: GERP, Genomic Evolutionary Rate Profiling; MAF, minor allele frequency; LOF, loss of function; ExAC (NFE), Exome Aggregation Consortium (Non-Finnish Europeans); SIFT, Sorting Intolerant From Tolerant.

<sup>a</sup>The following reference sequences were used in naming mutations. They correspond to RefSeq transcripts, unless otherwise specified: *GSTA5*, NM\_153699.1; *UNC5B*, NM\_170744.4; *BATF2*, NM\_001300807.1; *DPF2*, ENST00000531989 (from Ensembl; the variant is synonymous based on the RefSeq transcripts); *SART1*, NM\_005146.4; *KEAP1*, NM\_012289.3; *C19orf57*, NM\_024323.3; *ANGPTL6*, NM\_031917.2.

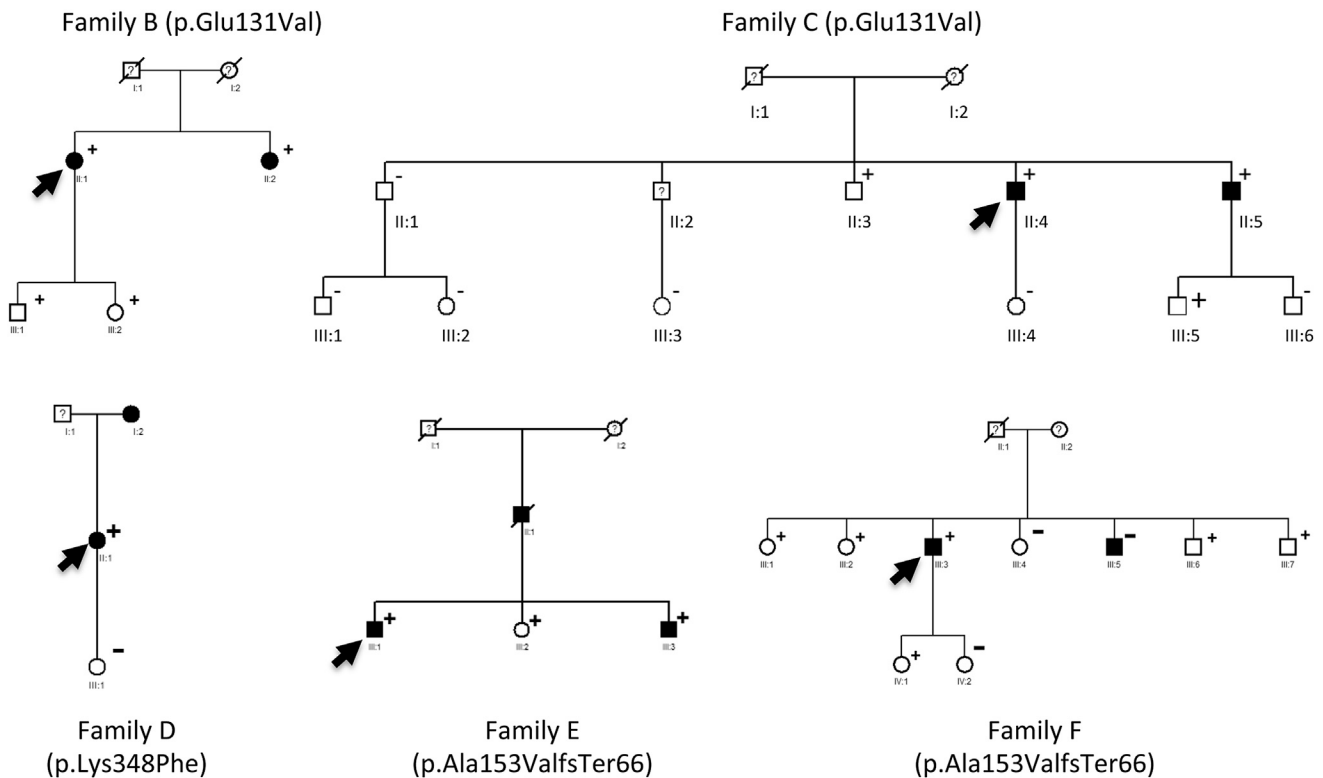


**Figure 2. Familial Case Subjects of IA in the Presence of Rare Coding Variants in *ANGPTL6***

Filled boxes, empty boxes, and boxes with question marks indicate IA-affected case subjects, non-affected relatives, and individuals with unknown status; plus sign (+) indicates the presence of the *ANGPTL6* variant; minus sign (-) indicates its absence; and black arrows indicate the index case subjects.

### Enrichment in Rare Coding Variants within *ANGPTL6* Among IA-Affected Case Subjects

We then extended genetic screening on the coding portion of *ANGPTL6* to 94 additional index case subjects with familial IA. We identified 5 additional individuals carrying rare, non-synonymous variants in *ANGPTL6* predicted as damaging *in silico* by PolyPhen-2 and/or SIFT (Table 1): two case subjects with the same missense mutation in exon 1 leading to the c.392A>T substitution (p.Glu131Val) in *ANGPTL6*, one case subject with a missense mutation in exon 4 leading to the c.1042C>T substitution (p.Leu348Phe), and two case subjects with the same CGCGCTGAGCCTCGGCGGA-bp insertion leading to one premature stop codon in exon 2 (c.439\_457dup [p.Ala153ValfsTer66]).

Overall, from the 6 index case subjects, family screening led to the identification of 16 relatives with diagnosed IAs (Tables 1 and S1; Figures 1A and 2). Out of the 13 family members carrying IAs and agreeing to participate in genetic research, 12 (92%) carry rare non-synonymous variants in *ANGPTL6* versus 15 out of 41 (34%) unaffected ones. The only affected individual who does not carry any rare coding variant in *ANGPTL6* is a 54-year-old male (III-5, family F, Figure 2) presenting with an aneurysm on the anterior communicant artery, with no reported history of smoking, high blood pressure, or any relevant associated disease.

The clinical characteristics of the remaining 12 case subjects are reported in Tables 2 and S1. Seven of them (58%) carry multiple IAs (with a maximum of three). IA is located on the middle cerebral artery bifurcation in 7 case subjects (58%), on the anterior communicant artery, the anterior cerebral artery, and the internal carotid artery in 3 case subjects (25%), and on the posterior communicant artery in 2 case subjects (17%).

To further test the association of *ANGPTL6* rare variants with susceptibility to familial IA, we also compared the proportions of individuals carrying at least one rare, non-synonymous variant across this gene among the 95 index case subjects enrolled in the present study (6/95; 6.32%) versus 404 healthy individuals with French ancestry (8/404; 1.98%). We found a significant enrichment in individuals carrying non-synonymous variants with an MAF below 1% in the NFE reference population, among IA-affected case subjects (SKAT,  $p = 0.023$ ; see Tables S2 and S3). Similar results were found when comparing allele counts among the 95 index case subjects versus the 7,509 non-Finnish European individuals with whole-genome sequences available in the gnomAD database (Tables S2 and S3).

### Reduced *ANGPTL6* Secretion in the Presence of the c.1378A>T Variant

*ANGPTL6* is one of the eight members of the secreted glycoprotein *ANGPTL* family, which share a common

**Table 2. Clinical Characteristics and Exposition to Risk Factors for IA-Affected Case Subjects and Unaffected Relatives, According to *ANGPTL6* Status**

	Healthy Individuals; No <i>ANGPTL6</i> Variant (n = 16 <sup>a</sup> )	Healthy Individuals; <i>ANGPTL6</i> Variant (n = 15)	IA Carriers; <i>ANGPTL6</i> Variant (n = 12)
Median age	57	56	59
Female sex	56%	53%	58%
History of smoking	56% (8 p.y. <sup>b</sup> )	73% (10 p.y. <sup>b</sup> )	67% (31 p.y. <sup>b</sup> )
High blood pressure	7%	9% <sup>c</sup>	50% <sup>c</sup>
Alcohol intake > 150 g/w	19%	13%	33%
Median BMI	22	24	24
Diabetes - dyslipidemia	19%	18%	33%

<sup>a</sup>Healthy individuals aged over 35 years, without *ANGPTL6* variant

<sup>b</sup>p.y., median consumption in pack/years among smokers

<sup>c</sup>Significant difference between affected versus healthy individuals carrying *ANGPTL6* variants; p = 0.013 (chi-square test)

structure consisting of an amino-terminal coiled-coil domain, a linker region, and a carboxy-terminal fibrinogen-like domain. The c.1378A>T *ANGPTL6* variant leads to the occurrence of a premature stop codon in the last exon. The corresponding transcript may thus escape the nonsense-mediated mRNA decay and is predicted to result in a protein truncated by the last 11 amino acids (p.Lys460Ter *ANGPTL6*). To analyze the functional properties of p.Lys460Ter *ANGPTL6*, we established stable cell lines expressing the wild-type (WT *ANGPTL6*) and mutant *ANGPTL6* (p.Lys460Ter *ANGPTL6*). The two types of cell lines expressed similar levels of transcripts suggesting that c.1378A>T *ANGPTL6* variant mRNA was not degraded (Figure 3A). Western blot using anti-FLAG antibody showed that WT *ANGPTL6* was secreted in the culture medium while p.Lys460Ter *ANGPTL6* was nearly undetectable in the supernatant of cells transfected with the variant (Figure 3B). Quantification of *ANGPTL6* concentration by ELISA confirmed the significant reduction of the secretion of p.Lys460Ter *ANGPTL6* compared to WT *ANGPTL6* (Figure 3B). In agreement with this defective secretion, immunofluorescence labeling and quantification in permeabilized cells clearly showed the retention of p.Lys460Ter *ANGPTL6* in the cytoplasm (Figure 3C). Although we did not directly demonstrate that c.1378A>T *ANGPTL6* variant mRNA escaped nonsense-mediated mRNA decay, our data strongly suggest that the c.1378A>T *ANGPTL6* variant leads to effective expression of the truncated p.Lys460Ter *ANGPTL6* protein, which is not secreted. Accordingly, heterozygous subjects for the c.1378A>T *ANGPTL6* variant are expected to present with decreased levels of circulating *ANGPTL6*. To assess this hypothesis, we performed ELISA to compare the serum concentration of *ANGPTL6* in subjects from family A reported as homozygous for the WT *ANGPTL6* (n = 5) versus

heterozygous for the c.1378A>T *ANGPTL6* (n = 7) and found a 50% reduction in the serum level of *ANGPTL6* in heterozygous subjects (Figure 3D).

A similar analysis of the serum concentration of *ANGPTL6* has been performed in subjects from family C. We found no reduction in the serum concentration of *ANGPTL6* between heterozygous subjects for p.Glu131Val *ANGPTL6* versus homozygous for the WT *ANGPTL6* (Figure S1).

## Discussion

In the present study, we identified one rare nonsense variant, c.1378A>T, in the last exon of angiopoietin-like 6 (*ANGPTL6*), which was carried by the four tested affected members of a large pedigree with multiple IA-affected case subjects. Because (1) the c.1378A>T nonsense variant is the only loss-of-function variant shared by all affected members in the family, (2) it is carried by only 5 out of the 22 unaffected relatives, and (3) *ANGPTL6* is a functionally relevant candidate for playing a role in IA pathophysiology, we thereafter focused our investigations on this particular gene.

Indeed, members of the *ANGPTL* family have been reported as regulators of angiogenesis through their carboxyl terminus.<sup>26</sup> In human, *ANGPTL6* has been identified as a circulating pro-angiogenic factor mainly secreted from the liver, which increases endothelial permeability and stimulates endothelial cell migration.<sup>27,28</sup> Although members of the *ANGPTL* family have also been described as regulators of glucose and lipoprotein metabolisms through their amino terminus,<sup>13</sup> a large-scale population study has shown that *ANGPTL6* does not affect lipoprotein profile.<sup>29</sup>

Interestingly, it is known that genes associated with vascular malformations of the brain have demonstrated or plausible roles in angiogenesis and vascular remodeling.<sup>30</sup> The development of the vasculature involves both vasculogenesis during embryogenesis and angiogenesis. Vasculogenesis of the cerebral vasculature occurs outside the brain, followed by capillary sprouting from the perineural plexus to penetrate the neural tube. Growth of the cerebral vasculature then entirely results from angiogenesis that requires vascular endothelial cell proliferation and migration, then vascular stabilization, corresponding to the formation of capillary tubes by endothelial cells and the recruitment of pericytes, the smooth muscle cell precursors, to their walls. All these timely organized events are tightly controlled by angiogenic factors, and aberrant expression or function of these mediators, including *ANGPTL6*, may lead to abnormal cerebral artery wall formation.<sup>31–33</sup> For example, defective recruitment of pericytes leads to vessel dilation and microaneurysm.<sup>31</sup>

We then extended our genetic screen on *ANGPTL6* to 94 additional index case subjects with familial IA and identified additional rare missense or frameshift variants in this

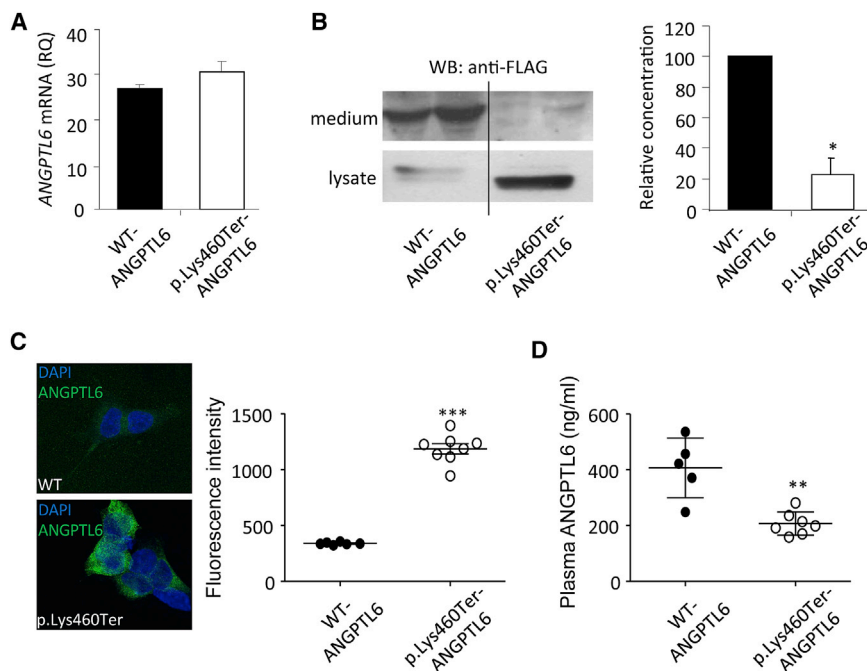


**Figure 3. Analysis of WT and p.Lys460Ter ANGPTL6 in Cultured Cells and Individual Sera**

(A) Analysis by qPCR of *ANGPTL6* transcripts in HEK293 cells encoding WT and p.Lys460Ter *ANGPTL6*.

(B) Analysis by western blot (anti-FLAG Ab) and ELISA of the levels of WT and p.Lys460Ter *ANGPTL6* in culture media and lysates from stably transfected HEK293.

(C) Immunofluorescence labeling with anti-*ANGPTL6* Ab and corresponding quantification in permeabilized HEK293 cells expressing WT and p.Lys460Ter *ANGPTL6*.

(D) Analysis of serum levels of *ANGPTL6* in control subjects (WT *ANGPTL6*) and individuals harboring the p.Lys460Ter *ANGPTL6* variant (heterozygous)

All results are expressed as means and error bars indicate standard deviation. Significant differences between independent groups were assessed by the Mann-Whitney test (\* $p < 0.05$ , \*\* $p < 0.01$ , \*\*\* $p < 0.001$ ).

gene carried by index case subjects from 5 additional families (Figure 2 and Table 1). In total, among the 6 families, 12 out of 13 (92%) family members carrying IA also carry such variants in *ANGPTL6*, versus 15 out of 41 (37%) unaffected ones. The only affected individual who does not carry any rare coding variant in *ANGPTL6* (III-5, family F; Figure 2) presents with an IA in the anterior communicating artery, a location where IAs have been reported with probably weaker heritability.<sup>34,35</sup>

By burden test, we showed a significant enrichment in rare non-synonymous variants within this gene in our population of 95 index case subjects with familial IA, compared to a reference population of 404 individuals with French ancestry. This result confirms that rare coding variants in *ANGPTL6* are associated with familial forms of IA.

In human, *ANGPTL6* is described as a circulating protein mainly secreted from the liver and acting as an endocrine factor in the peripheral tissues.<sup>36</sup> Here we showed a 50% reduction of *ANGPTL6* serum concentration in heterozygous c.1378A>T subjects compared to their relatives who do not carry the variant. Our results in stably transfected cell lines suggest that this reduction may be caused by the inability of the truncated protein lacking the last 11 amino acids (p.Lys460Ter *ANGPTL6*) to be secreted. In contrast, we showed that heterozygous subjects for the c.392A>T (p.Glu131Val) variant present with similar levels of circulating *ANGPTL6* as subjects who do not carry the variant. This result does not exclude that *ANGPTL6* may be associated with IA through dysfunction of the secreted form of the protein. We could not assess the levels of circulating *ANGPTL6* in the remaining IA-affected case subjects and relatives, due to sample unavailability (Table S1).

In this study, we have observed some individuals ( $n = 15$ ) carrying possibly deleterious variations in *ANGPTL6* but without IA at the moment of the study. Since all affected individuals in our study have been subjected to at least one environmental risk factor, it is possible that familial rare variants in *ANGPTL6* require additional inauspicious factors to trigger IA development. A prominent and well-established environmental factor associated with the IA formation is the history of high blood pressure.<sup>8</sup> Indeed, we found in our study a significant difference in the rate of case subjects with a history of high blood pressure in affected versus healthy individuals heterozygous for *ANGPTL6* variants (Table 2). We hypothesize that *ANGPTL6* variants render cerebral arterial wall vulnerable to deformation, thus promoting lesion formation and/or progression, when challenged with other deleterious genetic or environmental factors such as high blood pressure, either through direct mechanical effects on vessel walls or by triggering inflammation. In the present study, we have identified rare coding variants in *ANGPTL6* causally related to IA in 6 families with multiple affected relatives. Our results point to a novel pathogenic pathway for a disease whose etiology is still poorly understood. Currently no molecular test has been established to help the diagnosis of IA. Developing biomarkers could undoubtedly facilitate early detection and risk assessment of IA. In this context, correlating the activity level of *ANGPTL6* with IA risk could be of great interest. A knock-in mouse model is currently under development in order to address these prominent questions about *ANGPTL6* and IA susceptibility. Discovering genetic risk factors and better understanding the molecular mechanisms responsible for IA formation will be prerequisites for the identification of new therapeutic targets.

## Supplemental Data

Supplemental Data include one figure and three tables and can be found with this article online at <https://doi.org/10.1016/j.ajhg.2017.12.006>.

## Consortia

The ICAN Study Group includes the following investigators: Hubert Desal, Romain Bourcier, Benjamin Dumas-Duport, Bertrand Isidor, Jérôme Connault, Pierre Lebranchu, Thierry Le Tourneau, Marie Pierre Viarouge, Chrisanthi Papagiannaki, Michel Piotin, Hocine Redjem, Mikael Mazighi, Jean Philippe Desilles, Olivier Nagara, Denis Trystram, Myriam Edjlali-Goujon, Christine Rodriguez, Waghi Ben Hassen, Suzanna Saleme, Charbel Mounayer, Olivier Levrier, Pierre Aguetaz, Xavier Combaz, Anne Pasco, Emeline Berthier, Marc Bintner, Marc Molho, Pascale Gauthier, Cyril Chivot, Vincent Costalat, Cyril Darganzil, Alain Bonafé, Anne Christine Januel, Caterina Michelozzi, Christophe Cognard, Fabrice Bonneville, Philippe Tall, Jean Darcourt, Alessandra Biondi, Cristina Iosif, Elisa Pomerio, Jean Christophe Ferre, Jean Yves Gauvrit, François Eugene, Hélène Raoult, Jean Christophe Gentric, Julien Ognard, René Anxionnat, Serge Bracard, Anne Laure Derelle, Romain Tonnelet, Laurent Spelle, Léon Ikka, Robert Fahed, Aymeric Rouchaud, Augustin Ozanne, Jildaz Caroff, Nidal Ben Achour, Jacques Moret, Emmanuel Chabert, Jérôme Berge, Gaultier Marnat, Xavier Barreau, Florent Gariel, Frédéric Clarencon, Mohammed Aggour, Frédéric Ricolfi, Adrien Chavent, Pierre Thouant, Pablo Lebidinsky, Brivael Lemogne, Denis Herbreteau, Richard Bibi, Laurent Pierot, Sébastien Soize, Marc Antoine Labeyrie, Christophe Vandendries, Emmanuel Houdart, Appoline Kazemi, Xavier Leclerc, Jean Pierre Pruvo, Sophie Gallas, and Stéphane Velasco.

## Acknowledgments

We are grateful to the genomics and bioinformatics core facility (GenoBiRD) and to the cellular and tissue imaging core facility (MicroPICell) of Nantes for their expert services. We would like to thank the Genome Aggregation Database (gnomAD) and the groups that provided exome and genome variant data to this resource. A full list of contributing groups can be found at <http://gnomad.broadinstitute.org/about>. We acknowledge the Center of Biological Resources (CHU Nantes, Hôtel-Dieu, CBR, Nantes, France) as well as Martine and Marie-France Le Cunff and the Clinical Investigation Center 1413 of Nantes for their assistance in managing the ICAN and PREGO biobanks. This work was supported by the French Regional Council of Pays-de-la-Loire (VaCaRMe program to S.B., S.C., F.S., P.L., H.L.M., and R.R.), the Fondation Genavie (to G.L. and R.R.), the Agence Nationale de la Recherche (ANR-15-CE17-0008-01 to G.L.), the French Ministry of Health (clinical trial NCT02848495 to H.D.), the Société Française de Radiologie, and the Société française de Neuroradiologie (both to R.B.).

Received: July 28, 2017

Accepted: December 5, 2017

Published: January 4, 2018

## Web Resources

Ensembl Genome Browser, human genome, [http://useast.ensembl.org/Homo\\_sapiens/Info/Index](http://useast.ensembl.org/Homo_sapiens/Info/Index)

ExAC Browser, <http://exac.broadinstitute.org/>  
GenBank, <https://www.ncbi.nlm.nih.gov/genbank/>  
gnomAD Browser, <http://gnomad.broadinstitute.org/>  
OMIM, <http://www.omim.org/>  
Picard, <http://broadinstitute.github.io/picard/>  
PolyPhen-2, <http://genetics.bwh.harvard.edu/pph2/>  
RefSeq, <http://www.ncbi.nlm.nih.gov/RefSeq>  
SIFT, <http://sift.bii.a-star.edu.sg/>  
Variant Effect Predictor, [http://useast.ensembl.org/Homo\\_sapiens/Tools/VEP](http://useast.ensembl.org/Homo_sapiens/Tools/VEP)

## References

1. Vlak, M.H., Algra, A., Brandenburg, R., and Rinkel, G.J. (2011). Prevalence of unruptured intracranial aneurysms, with emphasis on sex, age, comorbidity, country, and time period: a systematic review and meta-analysis. *Lancet Neurol.* *10*, 626–636.
2. Laaksamo, E., Ramachandran, M., Frösen, J., Tulamo, R., Baumann, M., Friedlander, R.M., Harbaugh, R.E., Hernesniemi, J., Niemelä, M., Raghavan, M.L., and Laakso, A. (2012). Intracellular signaling pathways and size, shape, and rupture history of human intracranial aneurysms. *Neurosurgery* *70*, 1565–1572, discussion 1572–1573.
3. Nieuwkamp, D.J., Setz, L.E., Algra, A., Linn, F.H.H., de Rooij, N.K., and Rinkel, G.J.E. (2009). Changes in case fatality of aneurysmal subarachnoid haemorrhage over time, according to age, sex, and region: a meta-analysis. *Lancet Neurol.* *8*, 635–642.
4. Pierot, L., Spelle, L., Vitry, F.; and ATENA Investigators (2008). Immediate clinical outcome of patients harboring unruptured intracranial aneurysms treated by endovascular approach: results of the ATENA study. *Stroke* *39*, 2497–2504.
5. Huttunen, T., von und zu Fraunberg, M., Frösen, J., Lehecka, M., Tromp, G., Helin, K., Koivisto, T., Rinne, J., Ronkainen, A., Hernesniemi, J., and Jääskeläinen, J.E. (2010). Saccular intracranial aneurysm disease: distribution of site, size, and age suggests different etiologies for aneurysm formation and rupture in 316 familial and 1454 sporadic eastern Finnish patients. *Neurosurgery* *66*, 631–638, discussion 638.
6. Bacigaluppi, S., Piccinelli, M., Antiga, L., Veneziani, A., Passerini, T., Rampini, P., Zavanone, M., Severi, P., Tredici, G., Zona, G., et al. (2014). Factors affecting formation and rupture of intracranial saccular aneurysms. *Neurosurg. Rev.* *37*, 1–14.
7. Frösen, J. (2014). Smooth muscle cells and the formation, degeneration, and rupture of saccular intracranial aneurysm wall—a review of current pathophysiological knowledge. *Transl. Stroke Res.* *5*, 347–356.
8. Vlak, M.H.M., Rinkel, G.J.E., Greebe, P., and Algra, A. (2013). Independent risk factors for intracranial aneurysms and their joint effect: a case-control study. *Stroke* *44*, 984–987.
9. Bourcier, R., Redon, R., and Desal, H. (2015). Genetic investigations on intracranial aneurysm: update and perspectives. *J. Neuroradiol.* *42*, 67–71.
10. Alg, V.S., Sofat, R., Houlden, H., and Werring, D.J. (2013). Genetic risk factors for intracranial aneurysms: a meta-analysis in more than 116,000 individuals. *Neurology* *80*, 2154–2165.
11. Yasuno, K., Bakırcıoğlu, M., Low, S.-K., Bilgüvar, K., Gaál, E., Ruigrok, Y.M., Niemelä, M., Hata, A., Bijlenga, P., Kasuya, H., et al. (2011). Common variant near the endothelin receptor type A (EDNRA) gene is associated with intracranial aneurysm risk. *Proc. Natl. Acad. Sci. USA* *108*, 19707–19712.



12. Zhou, S., Ambalavanan, A., Rochefort, D., Xie, P., Bourassa, C.V., Hince, P., Dionne-Laporte, A., Spiegelman, D., Gan-Or, Z., Mirarchi, C., et al. (2016). RNF213 is associated with intracranial aneurysms in the French-Canadian population. *Am. J. Hum. Genet.* *99*, 1072–1085.
13. Santiago-Sim, T., Fang, X., Hennessy, M.L., Nalbach, S.V., DePalma, S.R., Lee, M.S., Greenway, S.C., McDonough, B., Hergenroeder, G.W., Patek, K.J., et al. (2016). *THSD1* (Thrombospondin Type 1 Domain Containing Protein 1) mutation in the pathogenesis of intracranial aneurysm and subarachnoid hemorrhage. *Stroke* *47*, 3005–3013.
14. Liu, W., Morito, D., Takashima, S., Mineharu, Y., Kobayashi, H., Hitomi, T., Hashikata, H., Matsuura, N., Yamazaki, S., Toyoda, A., et al. (2011). Identification of RNF213 as a susceptibility gene for moyamoya disease and its possible role in vascular development. *PLoS ONE* *6*, e22542.
15. Kamada, F., Aoki, Y., Narisawa, A., Abe, Y., Komatsuzaki, S., Kikuchi, A., Kanno, J., Niihori, T., Ono, M., Ishii, N., et al. (2011). A genome-wide association study identifies RNF213 as the first Moyamoya disease gene. *J. Hum. Genet.* *56*, 34–40.
16. Bourcier, R., Chatel, S., Bourcereau, E., Jouan, S., Marec, H.L., Dumas-Duport, B., Sevin-Allouet, M., Guillon, B., Roualdes, V., Riem, T., et al.; ICAN Investigators (2017). Understanding the pathophysiology of intracranial aneurysm: The ICAN Project. *Neurosurgery* *80*, 621–626.
17. Li, H., and Durbin, R. (2010). Fast and accurate long-read alignment with Burrows-Wheeler transform. *Bioinformatics* *26*, 589–595.
18. McKenna, A., Hanna, M., Banks, E., Sivachenko, A., Cibulskis, K., Kernytsky, A., Garimella, K., Altshuler, D., Gabriel, S., Daly, M., and DePristo, M.A. (2010). The Genome Analysis Toolkit: a MapReduce framework for analyzing next-generation DNA sequencing data. *Genome Res.* *20*, 1297–1303.
19. Lindenbaum, P., Le Scouarnec, S., Portero, V., and Redon, R. (2011). Knime4Bio: a set of custom nodes for the interpretation of next-generation sequencing data with KNIME. *Bioinformatics* *27*, 3200–3201.
20. Han, L., and Abney, M. (2011). Identity by descent estimation with dense genome-wide genotype data. *Genet. Epidemiol.* *35*, 557–567.
21. Karachachoff, M., Duforet-Frebourg, N., Simonet, F., Le Scouarnec, S., Pellen, N., Lecointe, S., Charpentier, E., Gros, F., Cauchi, S., Froguel, P., et al.; D E S I R Study Group (2015). Fine-scale human genetic structure in Western France. *Eur. J. Hum. Genet.* *23*, 831–836.
22. Wu, M.C., Lee, S., Cai, T., Li, Y., Boehnke, M., and Lin, X. (2011). Rare-variant association testing for sequencing data with the sequence kernel association test. *Am. J. Hum. Genet.* *89*, 82–93.
23. Morgenthaler, S., and Thilly, W.G. (2007). A strategy to discover genes that carry multi-allelic or mono-allelic risk for common diseases: a cohort allelic sums test (CAST). *Mutat. Res.* *615*, 28–56.
24. Lek, M., Karczewski, K.J., Minikel, E.V., Samocha, K.E., Banks, E., Fennell, T., O'Donnell-Luria, A.H., Ware, J.S., Hill, A.J., Cummings, B.B., et al.; Exome Aggregation Consortium (2016). Analysis of protein-coding genetic variation in 60,706 humans. *Nature* *536*, 285–291.
25. Thorvaldsdóttir, H., Robinson, J.T., and Mesirov, J.P. (2013). Integrative Genomics Viewer (IGV): high-performance genomics data visualization and exploration. *Brief. Bioinform.* *14*, 178–192.
26. Hato, T., Tabata, M., and Oike, Y. (2008). The role of angiopoietin-like proteins in angiogenesis and metabolism. *Trends Cardiovasc. Med.* *18*, 6–14.
27. Santulli, G. (2014). Angiopoietin-like proteins: a comprehensive look. *Front. Endocrinol. (Lausanne)* *5*, 4.
28. Oike, Y., Ito, Y., Maekawa, H., Morisada, T., Kubota, Y., Akao, M., Urano, T., Yasunaga, K., and Suda, T. (2004). Angiopoietin-related growth factor (AGF) promotes angiogenesis. *Blood* *103*, 3760–3765.
29. Romeo, S., Yin, W., Kozlitina, J., Pennacchio, L.A., Boerwinkle, E., Hobbs, H.H., and Cohen, J.C. (2009). Rare loss-of-function mutations in ANGPTL family members contribute to plasma triglyceride levels in humans. *J. Clin. Invest.* *119*, 70–79.
30. Leblanc, G.G., Golanov, E., Awad, I.A., Young, W.L.; and Biology of Vascular Malformations of the Brain NINDS Workshop Collaborators (2009). Biology of vascular malformations of the brain. *Stroke* *40*, e694–e702.
31. Hellström, M., Kalén, M., Lindahl, P., Abramsson, A., and Betsholtz, C. (1999). Role of PDGF-B and PDGFR-beta in recruitment of vascular smooth muscle cells and pericytes during embryonic blood vessel formation in the mouse. *Development* *126*, 3047–3055.
32. Raab, S., Beck, H., Gaumann, A., Yüce, A., Gerber, H.P., Plate, K., Hammes, H.P., Ferrara, N., and Breier, G. (2004). Impaired brain angiogenesis and neuronal apoptosis induced by conditional homozygous inactivation of vascular endothelial growth factor. *Thromb. Haemost.* *91*, 595–605.
33. Nguyen, H.L., Lee, Y.J., Shin, J., Lee, E., Park, S.O., McCarty, J.H., and Oh, S.P. (2011). TGF- $\beta$  signaling in endothelial cells, but not neuroepithelial cells, is essential for cerebral vascular development. *Lab. Invest.* *91*, 1554–1563.
34. Bourcier, R., Lenoble, C., Guyomarch-Delasalle, B., Dumas-Duport, B., Papagiannaki, C., Redon, R., and Desal, H. (2017). Is there an inherited anatomical conformation favoring aneurysmal formation of the anterior communicating artery? *J. Neurosurg.* *126*, 1598–1605.
35. Mackey, J., Brown, R.D., Jr., Moomaw, C.J., Hornung, R., Sauerbeck, L., Woo, D., Foroud, T., Gandhi, D., Kleindorfer, D., Flaherty, M.L., et al.; FIA Investigators (2013). Familial intracranial aneurysms: is anatomic vulnerability heritable? *Stroke* *44*, 38–42.
36. Oike, Y., Akao, M., Yasunaga, K., Yamauchi, T., Morisada, T., Ito, Y., Urano, T., Kimura, Y., Kubota, Y., Maekawa, H., et al. (2005). Angiopoietin-related growth factor antagonizes obesity and insulin resistance. *Nat. Med.* *11*, 400–408.

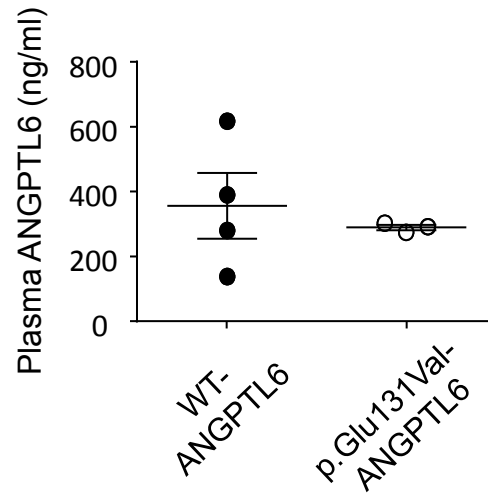
**Supplemental Data**

**Rare Coding Variants in *ANGPTL6* Are Associated  
with Familial Forms of Intracranial Aneurysm**

**Romain Bourcier, Solena Le Scouarnec, Stéphanie Bonnaud, Matilde Karakachoff, Emmanuelle Bourcereau, Sandrine Heurtebise-Chrétien, Céline Menguy, Christian Dina, Floriane Simonet, Alexis Moles, Cédric Lenoble, Pierre Lindenbaum, Stéphanie Chatel, Bertrand Isidor, Emmanuelle Génin, Jean-François Deleuze, Jean-Jacques Schott, Hervé Le Marec, ICAN Study Group, Gervaise Loirand, Hubert Desal, and Richard Redon**

## Supplemental Figure 1

Analysis of serum levels of ANGPTL6 in controls (WT-ANGPTL6) and individuals expressing the p.Glu131Val-ANGPTL6 (heterozygous).



Supplemental Table 2: Association tests on rare coding variants in *ANGPTL6*

Statistical test	Number of carriers		Allele count		p-value	OR	CI 95%
	IA cases	Internal controls	IA cases	gnomAD NFE individuals			
SKAT	6/95	8/404	-	-	0.0233	-	-
CAST	6/95	8/404	-	-	0.0331	3.326	[0.927-11.242]
FISHER	-	-	6/190	169/15018	0.0227	2.865	[1.023-6.485]

Supplemental Table 3: Full list of rare coding variants \* detected in *ANGPTL6* among IA cases and reference individuals

GRCh37/ hg19 position	rsID	REF allele	ALT allele	Protein Consequence (ENSP00000253109)	Transcript Consequence (ENST00000253109)	Annotation	Allele Count in cases (n=95)	Allele Count in internal controls (n=404)	Allele Count (gnomAD NFE)	MAF (gnomAD NFE)
19:10203293	.	G	C	p.Ala462Gly	c.1385C>G	missense	0	0	1	6.68E-05
19:10203300	rs769022609	T	A	p.Lys460Ter	c.1378A>T	stop gained	1	0	0	-
19:10203324	rs200825170	G	A	p.Arg452Cys	c.1354C>T	missense	0	0	1	6.68E-05
19:10203363	rs201518909	G	A	p.Arg439Ter	c.1315C>T	stop gained	0	0	2	1.33E-04
19:10203375	rs150235799	C	T	p.Gly435Ser	c.1303G>A	missense	0	0	1	6.67E-05
19:10203390	rs769478685	C	T	p.Gly430Ser	c.1288G>A	missense	0	0	1	6.67E-05
19:10203416	rs548381762	T	C	p.His421Arg	c.1262A>G	missense	0	0	1	6.69E-05
19:10203432	rs146282548	C	G	p.Gly416Arg	c.1246G>C	missense	0	1	9	6.02E-04
19:10203434	rs372960335	C	T	p.Arg415Gln	c.1244G>A	missense	0	1	1	6.69E-05
19:10203435	rs377498859	G	A	p.Arg415Trp	c.1243C>T	missense	0	0	1	6.69E-05
19:10203444	.	G	C	p.Leu412Val	c.1234C>G	missense	0	0	2	1.34E-04
19:10204027	rs776568403	G	T	p.Ser407Tyr	c.1220C>A	missense	0	0	1	6.67E-05
19:10204052	rs568396237	C	T	p.Val399Met	c.1195G>A	missense	0	0	1	6.67E-05
19:10204083	.	AAGAG	A	p.Ser387PhefsTer81	c.1160_1163delCTCT	frameshift	0	0	1	6.67E-05
19:10204132	.	T	C	p.His372Arg	c.1115A>G	missense	0	0	1	6.67E-05
19:10204137	rs761235613	G	T	p.Ser370Arg	c.1110C>A	missense	0	0	1	6.67E-05
19:10204142	rs754265148	C	T	p.Glu369Lys	c.1105G>A	missense	0	0	1	6.67E-05
19:10204187	rs779222736	C	G	p.Gly354Arg	c.1060G>C	missense	0	0	3	2.00E-04
19:10204205	.	G	A	p.Leu348Phe	c.1042C>T	missense	1	0	0	-
19:10204215	rs769287477	C	G	p.Glu344Asp	c.1032G>C	missense	0	1	0	-
19:10204229	rs138652863	G	A	p.Arg340Cys	c.1018C>T	missense	0	0	3	2.00E-04
19:10204239	.	C	G	p.Gln336His	c.1008G>C	missense	0	0	1	6.67E-05
19:10204377	.	G	C	p.His315Asp	c.943C>G	missense	0	0	1	6.66E-05
19:10204419	rs748744561	G	A	p.Arg301Trp	c.901C>T	missense	0	0	2	1.33E-04
19:10204440	rs201494217	C	T	p.Gly294Arg	c.880G>A	missense	0	0	1	6.66E-05
19:10204464	rs774043154	A	G	p.Trp286Arg	c.856T>C	missense	0	0	2	1.33E-04
19:10204469	rs201622589	G	C	p.Ser284Ter	c.851C>G	stop gained	0	0	24	1.60E-03
19:10204476	rs760163416	C	T	p.Val282Ile	c.844G>A	missense	0	0	1	6.66E-05
19:10204510	rs778164883	C	A	p.Gln270His	c.810G>T	missense	0	0	1	6.67E-05
19:10204512	rs372998779	G	C	p.Gln270Glu	c.808C>G	missense	0	0	3	2.00E-04
19:10204529	rs150117768	C	A	p.Arg264Leu	c.791G>T	missense	0	0	1	6.67E-05
19:10204530	rs182345321	G	A	p.Arg264Cys	c.790C>T	missense	0	0	5	3.33E-04
19:10205491	.	C	T	p.Glu236Lys	c.706G>A	missense	0	0	2	1.33E-04
19:10205553	rs138519545	T	C	p.Asp215Gly	c.644A>G	missense	0	0	1	6.66E-05
19:10205607	rs145558307	G	A	p.Pro197Leu	c.590C>T	missense	0	0	1	6.67E-05
19:10206662	rs200836122	T	C	p.Gln193Arg	c.578A>G	missense	0	0	13	8.68E-04
19:10206680	rs771739756	C	G	p.Gly187Ala	c.560G>C	missense	0	0	1	6.72E-05
19:10206686	.	C	A	p.Cys185Phe	c.554G>T	missense	0	0	1	6.68E-05
19:10206729	.	C	G	p.Val171Leu	c.511G>C	missense	0	1	0	-
19:10206761	rs771917209	A	C	p.Leu160Arg	c.479T>G	missense	0	0	1	6.70E-05
19:10206763	rs369847598	C	A	p.Gln159His	c.477G>T	missense	0	0	5	3.35E-04
19:10206774	rs770895499	G	A	p.Arg156Trp	c.466C>T	missense	0	0	1	6.72E-05
19:10206780	rs199549770	C	T	p.Ala154Thr	c.460G>A	missense	0	0	1	6.72E-05
19:10206782	rs770263825	G	GCGCGCTGAG CCTCGGCGGA	p.Ala153ValfsTer66	c.439_457dupTCCGCC GAGGCTCAGCGCG	frameshift	2	0	1	6.72E-05
19:10206787	rs776060868	C	CTGAGCCTCGG CGGACGCGT	p.Ala153ValfsTer66	c.434_452dupACGCGT CCGCCGAGGCTCA	frameshift	0	0	2	1.34E-04
19:10206801	rs779899913	A	G	p.Ser147Pro	c.439T>C	missense	0	0	1	6.76E-05
19:10206824	rs554909694	A	G	p.Leu139Pro	c.416T>C	missense	0	0	1	6.82E-05
19:10206824	rs554909694	A	T	p.Leu139His	c.416T>A	missense	0	0	1	6.82E-05

19:10206848	rs576667683	T	A	p.Glu131Val	c.392A>T	missense	2	2	39	2.67E-03
19:10206854	.	C	G	p.Gly129Ala	c.386G>C	missense	0	1	0	-
19:10206875	.	G	A	p.Ala122Val	c.365C>T	missense	0	0	1	6.92E-05
19:10206896	.	T	C	p.Gln115Arg	c.344A>G	missense	0	0	1	6.94E-05
19:10206915	.	G	A	p.Gln109Ter	c.325C>T	stop gained	0	0	1	7.00E-05
19:10206993	.	C	A	p.Ala83Ser	c.247G>T	missense	0	0	1	6.82E-05
19:10206995	.	A	T	p.Leu82Gln	c.245T>A	missense	0	0	1	6.81E-05
19:10206997	.	C	G	p.Arg81Ser	c.243G>C	missense	0	1	3	2.03E-04
19:10207001	.	T	C	p.Gln80Arg	c.239A>G	missense	0	0	1	6.77E-05
19:10207020	.	C	G	p.Glu74Gln	c.220G>C	missense	0	0	1	6.73E-05
19:10207035	.	C	T	p.Val69Ile	c.205G>A	missense	0	0	3	2.05E-04
19:10207035	.	C	A	p.Val69Phe	c.205G>T	missense	0	0	1	6.82E-05
19:10207053	.	C	G	p.Ala63Pro	c.187G>C	missense	0	0	2	1.35E-04
19:10207059	.	C	T	p.Glu61Lys	c.181G>A	missense	0	0	1	6.76E-05
19:10207076	rs560311003	T	G	p.Glu55Ala	c.164A>C	missense	0	0	1	6.77E-05
19:10207083	rs746538090	T	A	p.Thr53Ser	c.157A>T	missense	0	0	1	6.76E-05
19:10207103	rs560892001	C	T	p.Gly46Asp	c.137G>A	missense	0	0	2	1.34E-04
19:10207104	.	C	T	p.Gly46Ser	c.136G>A	missense	0	0	1	6.73E-05
19:10207225	rs751565560	C	T	p.Trp5Ter	c.15G>A	stop gained	0	0	1	6.69E-05

\* Rare variants were defined as having an MAF below 1% among the whole-genome sequenced individuals with European Non-Finnish ancestry available in gnomAD